The Plant Cell, Vol. 18, 688–698, March 2006, www.plantcell.org

The Free NADH Concentration Is Kept Constant in Plant Mitochondria under Different Metabolic Conditions

Marina R. Kasimova,[a] Jurgita Grigiene,[b] Klaas Krab,[c] Peter H. Hagedorn,[d] Henrik Flyvbjerg,[d] Peter E. Andersen,[a] and Ian M. Møller[e,1]

[a] Optics and Plasma Research Department, Risø National Laboratory, DK-4000 Roskilde, Denmark
[b] Laboratory of Biochemistry, Institute for Biomedical Research, Kaunas University of Medicine, LT-3009 Kaunas, Lithuania
[c] Department of Molecular Cell Physiology, Earth, and Life Sciences, Vrije Universiteit, 1081 HV Amsterdam, The Netherlands
[d] Biosystems Department, Risø National Laboratory, DK-4000 Roskilde, Denmark
[e] Department of Agricultural Sciences, Royal Veterinary and Agricultural University, DK-1871 Frederiksberg C, Denmark

The reduced coenzyme NADH plays a central role in mitochondrial respiratory metabolism. However, reports on the amount of free NADH in mitochondria are sparse and contradictory. We first determined the emission spectrum of NADH bound to proteins using isothermal titration calorimetry combined with fluorescence spectroscopy. The NADH content of actively respiring mitochondria (from potato tubers [*Solanum tuberosum* cv Bintje]) in different metabolic states was then measured by spectral decomposition analysis of fluorescence emission spectra. Most of the mitochondrial NADH is bound to proteins, and the amount is low in state 3 (substrate + ADP present) and high in state 2 (only substrate present) and state 4 (substrate + ATP). By contrast, the amount of free NADH is low but relatively constant, even increasing a little in state 3. Using modeling, we show that these results can be explained by a 2.5- to 3-fold weaker average binding of NADH to mitochondrial protein in state 3 compared with state 4. This indicates that there is a specific mechanism for free NADH homeostasis and that the concentration of free NADH in the mitochondrial matrix per se does not play a regulatory role in mitochondrial metabolism. These findings have far-reaching consequences for the interpretation of cellular metabolism.

INTRODUCTION

NAD and NADP are two of the most used coenzymes in cellular metabolism. More than 500 known enzymes use NAD(P) to catalyze reduction-oxidation reactions reversibly (Enzyme Nomenclature; http://www.chem.qmul.ac.uk/iubmb/enzyme). Some of these are among the most abundant and well-studied enzymes participating in energy metabolism (glycolysis, the Krebs cycle, the Calvin cycle), biosynthesis, degradation, defense against oxidative damage, etc. NAD(P) is found in mitochondria, chloroplasts, peroxisomes, the cytosol, and other cellular compartments, typically at a total concentration of one to several millimolar.

The reduced and oxidized forms of the two coenzymes have distinct spectroscopic characteristics—NAD(P)H is fluorescent, while its oxidized form is not. Furthermore, the fluorescence properties of bound and free NAD(P)H also differ. Free NADH has an emission peak at 460 nm and a lifetime of 0.4 ns (Scott et al., 1970; Gafni and Brand, 1976; Lakowics et al., 1992), whereas the emission maximum of the NADH bound to proteins is shifted to 430 to 435 nm, its lifetime is severalfold longer, and the fluorescence intensity is higher (Duysens and Kronenberg, 1957; Langan, 1960; Avi-Dor et al., 1962; Wakita et al., 1995). Several methods are available for measuring the amount of NAD(P) in organelles, cells, and tissues. Total NAD(P) can be extracted and quantified (e.g., by enzymatic methods or by HPLC analysis) (Stocchi et al., 1985; Agius et al., 2001). Total NAD(P)H in situ can be monitored, but not easily quantified, by fluorescence spectrophotometry. Combining extraction and equilibrium considerations, it is possible to calculate the concentrations of free NAD(P)H, the relevant parameter for the interaction of the coenzyme with enzymes. However, this is difficult and not easily verifiable. Finally, Paul and Schneckenburger (1996) introduced a fluorometric method whereby a 2-ns pulse of 355-nm light was used to excite a sample containing both free and bound NADH, and the amount of free NADH was measured as a 460-nm emission 0 to 5 ns after the pulse and bound NADH as a 430-nm emission 5 to 10 ns after the pulse. However, the spectra of free and bound NADH overlapped, and no attempt was made to make the method quantitative.

Despite the importance of NAD(P) in mitochondrial metabolism, little is known about the amount of free NAD(P)H, the parameter important for the interaction of the coenzyme with enzymes. Wakita et al. (1995) were unable to detect free NADH in rat liver mitochondria using fluorescence decay analysis. This implies that a small proportion of the total NADH is free. By contrast, Blinova et al. (2005) reported a high relative concentration of free NADH in pig heart mitochondria. This disagreement between the reports of different groups is a basis for confusion about the role of free NADH in mitochondrial metabolism. The purpose of our work was both to verify the presence of free

[1] To whom correspondence should be addressed. E-mail imm@kvl.dk; fax 45-3528-3460.
The author responsible for distribution of materials integral to the findings presented in this article in accordance with the policy described in the Instructions for Authors (www.plantcell.org) is: Ian M. Møller (imm@kvl.dk).
Article, publication date, and citation information can be found at www.plantcell.org/cgi/doi/10.1105/tpc.105.039354.

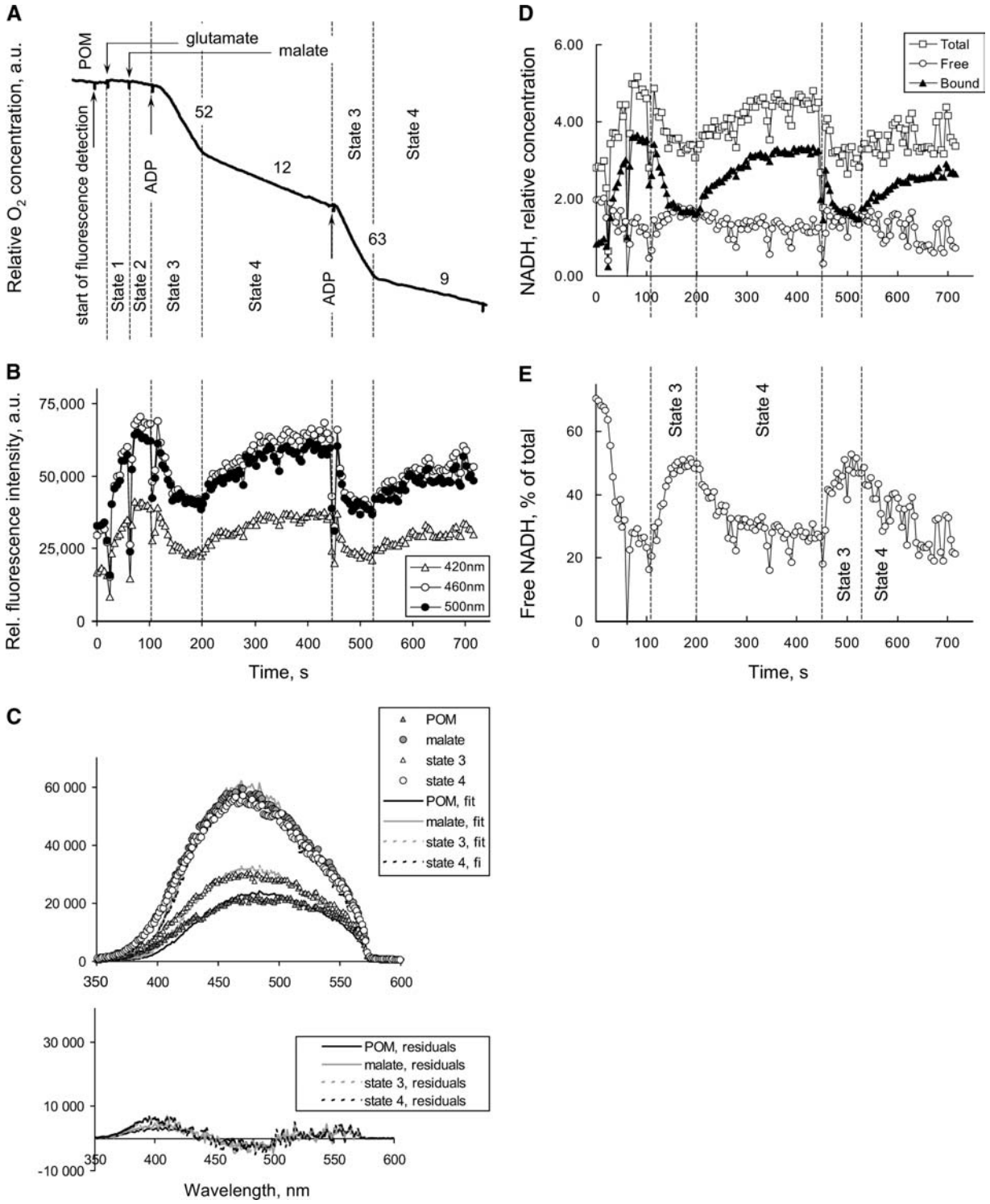

Figure 1. Analysis of Free and Bound NADH in Isolated Potato Tuber Mitochondria Oxidizing Malate (+Glu).

(A) Oxygen consumption during states 1, 2, 3-4, and 3-4. Additions were as follows (in final concentrations): mitochondria (0.91 mg/mL), Glu (10 mM), malate (25 mM), and ADP (0.3 mM twice). Numbers along the traces are rates of oxygen consumption in nmol/min × mg protein. a.u., arbitrary units.
(B) Fluorescence at 420, 460, and 500 nm as a function of time.
(C) Fluorescence spectra from selected time points (state 1, 9.6 s; state 2, 96 s; state 3, 196.8 s; state 4, 422.4 s) with the fits and the residuals.
(D) Amounts in arbitrary units of free, bound, and total NADH obtained by decomposition of the fluorescence spectra.
(E) Free NADH as a percentage of total NADH.
Uncorrected spectra are shown in **(B)** and **(C)** (see Figure 7).

Table 1. NAD(H) in Potato Tubers Estimated by Extraction

Incubation Conditions	Amount (nmol/mg protein)[a]			
	NADH	NAD^+	Total	Reduction (%)
POM (state 1)	0.02 ± 0.05	1.00 ± 0.31	1.03 ± 0.35	3 ± 3
POM + mal + glut (state 2)[b]	0.47 ± 0.07	0.73 ± 0.30	1.19 ± 0.37	40 ± 5
POM + mal + glut + ADP (state 3)	0.24 ± 0.20	0.96 ± 0.37	1.19 ± 0.57	18 ± 7
POM + mal + glut + ATP (state 4)	0.48 ± 0.31	0.74 ± 0.26	1.23 ± 0.55	37 ± 10

Total NAD^+ and NADH were extracted from potato tuber mitochondria (POM) oxidizing malate + Glu in different metabolic states.
[a] Numbers are given as mean ± SD ($n = 3$ independent preparations of mitochondria).
[b] mal + glut, 25 mM malate + 10 mM Glu.

NADH in mitochondria and to investigate its role in the regulation of respiratory processes.

RESULTS

Mitochondrial Respiration with Malate (+Glu) as Substrate

Isolated potato (*Solanum tuberosum* cv Bintje) tuber mitochondria were incubated in a respiratory medium, and substrate and ADP were added consecutively. In the following work, we will use the nomenclature for respiratory states of isolated mitochondria introduced by Chance and Williams (see Nicholls and Ferguson, 2002): State 1, mitochondria alone; state 2, only substrate added; state 3, substrate and a limited amount of ADP added; state 4, substrate and ATP added (or all ADP converted into ATP).

The oxygen consumption traces show the expected pattern (Figure 1A): There was little or no oxygen consumption until substrate was added. The mitochondria started respiring after the addition of substrate (Glu + malate; state 2), but the rate of oxidation was greatly enhanced when ADP was added (state 3). When the ADP was exhausted, the rate of oxidation became approximately fourfold slower (state 4), indicating that electron transport and ATP synthesis were well coupled in these mitochondria. After further addition of ADP, the pattern was repeated. In the example shown in Figure 1A, both states 3 and 4 were linear. However, state 4 sometimes showed two phases, slowest in the first half and faster after 2 to 3 min. This is well known for plant mitochondria oxidizing malate, and it is due to accumulation of oxaloacetate in state 3 and its removal in state 4 (Møller and Palmer, 1982; Palmer et al., 1982; Hagedorn et al., 2004). The linearity of state 4 shows that little oxaloacetate accumulated due to the presence of Glu. The concentrations of oxaloacetate and NADH in the matrix of plant mitochondria are intimately linked through the equilibrium of malate dehydrogenase (MDH) (Palmer et al., 1982; Møller and Lin, 1986; Hagedorn et al., 2004).

NADH Fluorescence during Malate Oxidation

The amount of free and bound NADH was monitored by exciting the mitochondria with nanosecond laser pulses at 355 nm and monitoring the fluorescence through the wall of the oxygen electrode vessel (see Methods). Emission spectra were collected every 4 s, and the data at 420, 460, and 500 nm are shown in Figure 1B as a function of time. Note that uncorrected spectra and uncorrected wavelengths are given here and elsewhere in Results. As demonstrated in Methods, the corrected peaks are blue-shifted by ~30 nm.

Upon addition of Glu and malate, the level of fluorescence intensity increased sharply at all wavelengths. The addition of ADP caused fluorescence to decrease throughout the spectrum but more so in the blue region. At the time of transition from state 3 to state 4 at 200 s, the fluorescence started increasing and reached the state 2 levels after a couple of minutes. This fluorescence response is perfectly consistent with the data obtained at fixed wavelengths in earlier investigations (Neuburger et al., 1984).

A puzzling feature of our data recurring in most of the samples was the initial fluorescence shown by mitochondria prior to the addition of substrates. The shape of these emission spectra was characteristic of the free NADH. However, extraction and quantification of NAD^+ and NADH by an analytical method showed clearly the absence of NADH in state 1, a high amount in states 2 and 4, and a low amount in state 3 (Table 1). Excitation fluorescence spectra of the mitochondria (data not shown) in state 1 also confirmed that they contained no NADH. This initial fluorescence is not associated with NADPH because no NADPH is detectable in isolated potato tuber mitochondria under any metabolic conditions (Agius et al., 2001).

Upon binding to a protein, the NADH emission maximum shifts to shorter wavelengths, while the fluorescence intensity increases fourfould to fivefold (see Methods; Duysens and Kronenberg, 1957; Langan, 1960; Avi-Dor et al., 1962; Wakita et al., 1995). The fluorescence spectra of potato tuber mitochondria,

Table 2. Comparison of the Total Amount of NADH in Potato Tuber Mitochondria Estimated by Extraction and by Fluorescence Spectral Decomposition

Conditions	Estimated by Extraction (nmol/mg protein)[a]	Estimated by Fluorescence (a.u.)[b]
State 2 (mal + glut)	0.47	100
State 3 (mal + glut + ADP)	0.24	56 ± 18
State 4 (mal + glut + ATP)	0.48	92 ± 2

[a] Data from Table 1.
[b] Numbers are given as mean ± SD ($n = 3$ independent preparations of mitochondria).

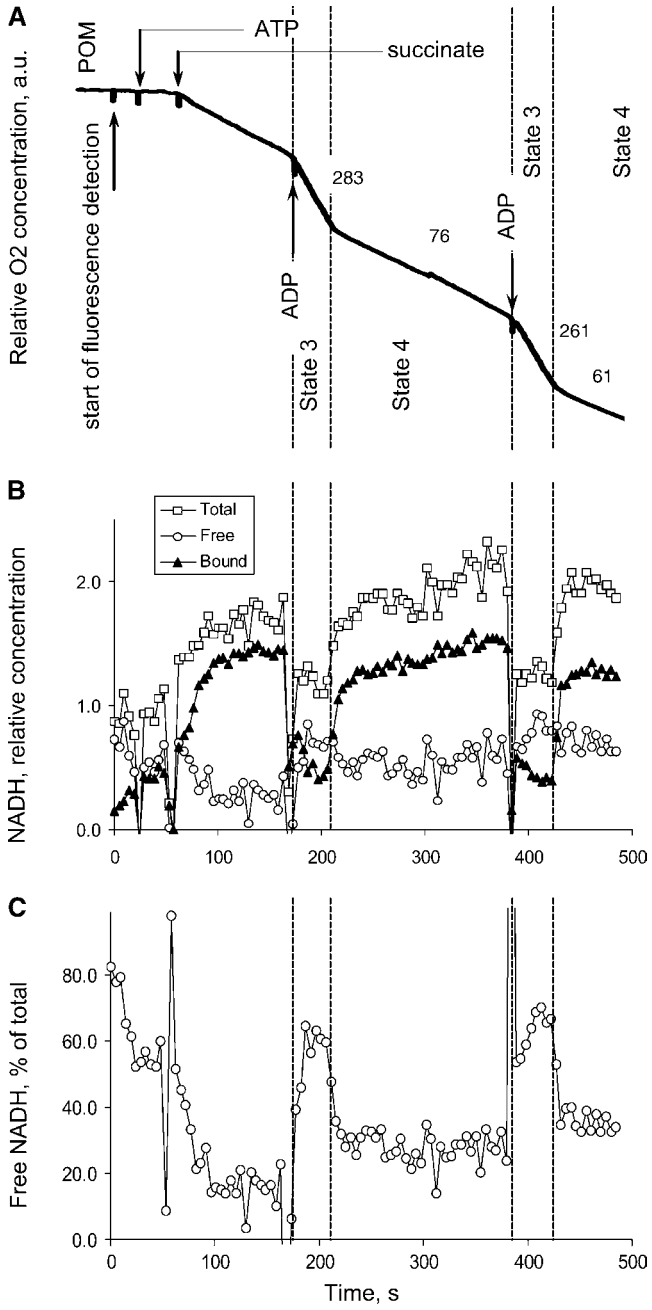

Figure 2. The Amounts of Total, Free, and Bound NADH in Isolated Potato Tuber Mitochondria Oxidizing Succinate.

Additions were as follows (in final concentrations): mitochondria (0.29 mg/mL), ATP (0.6 mM to activate succinate dehydrogenase), succinate (13 mM), and ADP (0.2 mM twice).

(A) Oxygen consumption during states 1, 2, 3-4, and 3-4. Numbers along the traces are rates of oxygen consumption in nmol/min × mg protein.

(B) Amounts in arbitrary units of free, bound, and total NADH obtained by deconvolutions of the fluorescence spectra.

(C) Free NADH as a percentage of total NADH.

uncorrected for the instrument intensity response function, are shown in Figure 1C. After correction for instrument response, the emission maximum for free NADH is at 460 to 470 nm, perfectly consistent with the literature (see Methods).

Upon addition of Glu + malate (state 2), the fluorescence intensity increased twofold (Figures 1B and 1C), and the emission peak blue-shifted ~30 nm, indicating that the proportion of bound NADH had increased. In state 3, the emission intensity decreased and the peak red-shifted, indicating a reversal of the effect of state 2. Finally, the emission spectrum in state 4 was very similar to that of state 2 (Figure 1C).

Determination of the Fluorescence Spectrum of Bound NADH in Respiring Mitochondria

To obtain the spectrum of NADH bound to mitochondrial matrix proteins, we used a model system consisting of NADH and alcohol dehydrogenase (ADH). The binding properties of this model were determined by isothermal titration calorimetry (ITC; see Methods). These binding parameters were used in analysis of fluorescence spectra of NADH/ADH mixtures for calculation of the spectrum of bound NADH. Using the spectra of the two NADH components, it was possible to fit the fluorescence spectra of mitochondria (see Figure 1C). A small, but distinct, deviation of the fitted curves from the experimental data indicates the presence of an additional component not accounted for in our model. A similar phenomenon was observed by French et al. (1998) in porcine heart mitochondria. Below 420 nm they detected a signal not associated with NADH fluorescence, which was ascribed to the excitation source bleed through. If a similar scattering component is introduced in our fitting data, the plot of deviation (Figure 1C, bottom panel) becomes essentially flat (M.R. Kasimova, unpublished data).

Changes in Bound and Free NADH in Response to Respiratory State

Total NADH displays a pattern similar to the fluorescence pattern (cf. Figures 1B and 1D), and it is consistent with the amounts of extracted NADH (Table 2). There was no bound NADH in state 1, but it increased sharply upon addition of respiratory substrate (state 2) to constitute the major part of total NADH (Figure 1D).

Table 3. Total Amounts of NADH and NAD^+ Were Measured by Extraction

	State 3 (μM)	State 4 (μM)
$[NADH]_{free}$	82	62
$[NADH]_{bound}$	82	160
$[NADH]_{total}$	160	220
$[NAD^+]_{total}$	730	640

The values used are specifically those for the same mitochondrial preparation used in Figure 1. The measurement of total NADH was used to convert free, bound, and total NADH as estimated from Figure 1D (state 3, ~190 s; state 4, ~420 s) from relative concentrations to micromolar in the matrix (1 mg mitochondrial protein is assumed to have 1 μL matrix volume).

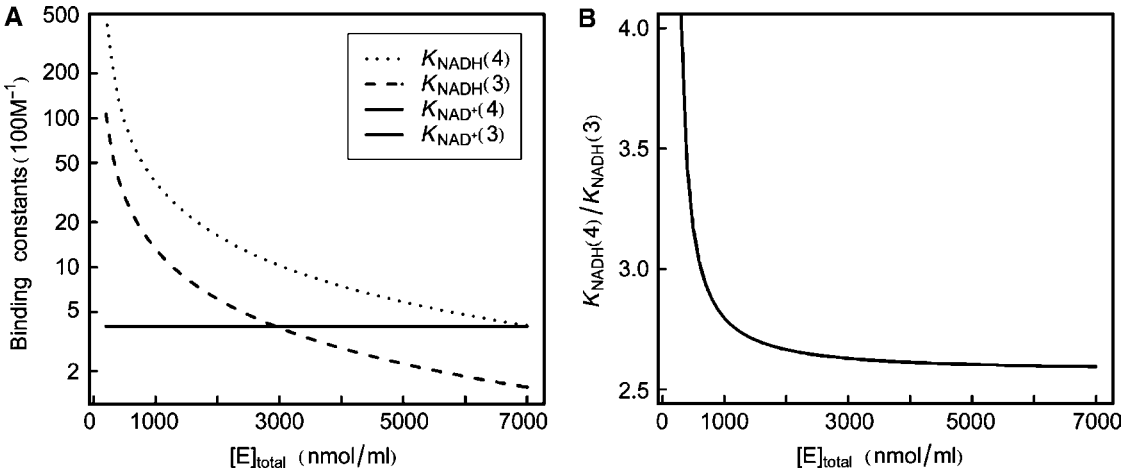

Figure 3. Modeling Results Showing the Fitted Binding Constants.

(A) Binding constants as a function of total amount of binding sites as found by fitting.
(B) The ratio of fitted binding constants, $K_{NADH}(4)$:$K_{NADH}(3)$, as a function of total amount of binding sites.

The amount of bound NADH responded in the same way as total NADH during the state 3/state 4 cycles. By sharp contrast, free NADH was almost invariable, showing only a slight increase in state 3 and a decrease back to the lower level during state 4 (Figure 1D). Accordingly, the relative contribution of free NADH varied markedly during the experiment (Figure 1E). In states 2 and 4, only a small part (20%) of total NADH was free, which is more consistent with the observations of Wakita et al. (1995). However, approximately half of NADH was free in state 3, which is similar to the estimations made by Blinova et al. (2005).

The transition in respiration between state 3 and state 4, as monitored by oxygen consumption, was rapid. Upon exhaustion of ADP, it took <20 s for the rate of oxygen consumption to reach a new steady state. Likewise, the faster linear state 3 rate was attained very quickly after ADP addition (Figure 1A). Clearly, the closure of the proton-conducting pore of the ATP synthase and the subsequent rise in the size of the membrane potential had an immediate effect upon the rate of electron transfer to oxygen. By contrast, the amount of NADH took ~2 min to reach its new steady state after the state 3/state 4 transition (Figure 1D). This is due to the presence of small amounts of oxaloacetate and the slow return of the MDH equilibrium (Hagedorn et al., 2004).

The changes in total, bound, and free NADH during succinate oxidation are shown in Figure 2. Here, the same pattern was observed as for malate oxidation except that the changes in NADH during the state 3/state 4 transitions were more rapid, reflecting the fact that no oxaloacetate was produced and that MDH was not involved in the reactions (Hagedorn et al., 2004). The time-dependent changes in NADH concentration during succinate oxidation reported here are very similar to those observed for the reduction level of the ubiquinone pool during succinate oxidation (Moore et al., 1988).

The disappearance of the fluorescence signal coming from bound NADH can be due to two processes: (1) Its conversion to NAD^+, which is not fluorescent and hence not detectable by our method and/or (2) its release from the binding site of an enzyme. With the increased respiration rate in state 3, more NADH is oxidized, leading to a lower steady state level of bound NADH (Hagedorn et al., 2004). Under equilibrium conditions, the free NADH concentration would readjust accordingly (i.e., decrease),

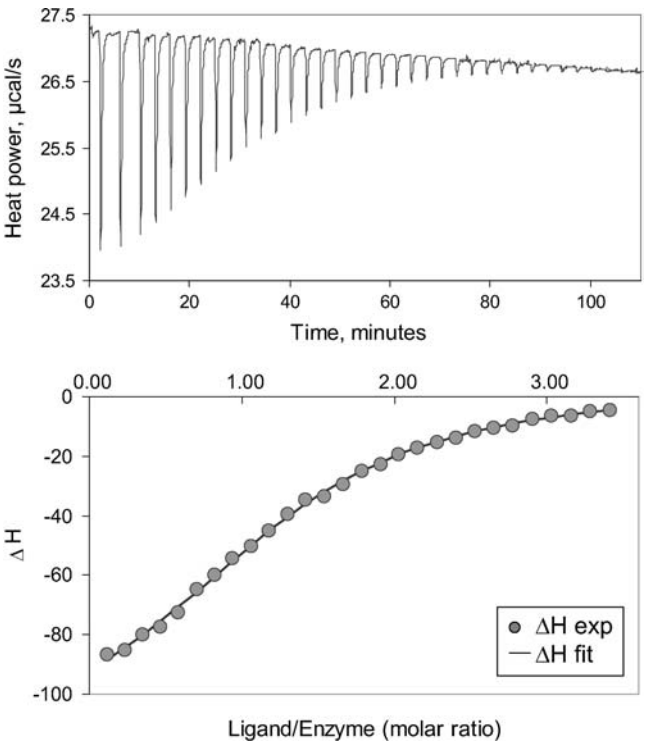

Figure 4. ITC Experiment Used for Determination of the Binding Constant of NADH to ADH.

Top panel, raw data; bottom panel, experimental heats and a fitted curve. See Table 4 for the fitting parameters.

Table 4. The Binding Parameters of Different NADH/Protein Systems Measured by ITC at 25°C and pH 7.5

Protein	k_a (1/M)	ΔH (kJ/mol)	*n*
MDH[a]	$6.57 \cdot 10^5$	−56.56	1.44
ADH[b]	$3.94 \cdot 10^4$	−57.22	1.23
BSA	$8.70 \cdot 10^3$	−56.72	0.74

[a] Mitochondrial MDH.
[b] Yeast ADH.

but this does not happen. Surprisingly, the concentration of free NADH remains relatively constant in state 3 (Figures 1D and 2B), leading to a large increase in the proportion of free NADH (Figures 1E and 2C). We have attempted to explain this phenomenon by modeling NADH and NAD^+ binding to mitochondrial proteins.

Modeling

The model is presented in Methods. Steady state relative concentrations of free, bound, and total NADH were estimated from Figure 1D. Total amounts of NADH and NAD^+ were measured by extraction (Table 1). The estimated relative concentration of total NADH was compared with the measurement of extracted total NADH (Table 2). Using this comparison, relative concentrations of free and bound NADH were converted to absolute concentrations accordingly. The concentrations are given in Table 3.

Assuming that states 3 and 4 are both in steady state, we wish to determine sets of parameters for each state that reproduce the data in Table 3—the most interesting aspect being the slight increase in the amount of free NADH from state 4 to state 3.

There are five parameters: *n*, *e*, K_C, K_{NADH}, and K_{NAD^+}. The extractions (Table 1) show that the total concentration of NAD(H) (*n*) does not change between states. Likewise, the total concentration of proteins binding NAD(H) (i.e., the total number of binding sites [*e*]), is also constant, whereas the binding strength may vary (see below). The parameter K_C represents a combination of a number of enzyme reactions, some of which are known to change between states 3 and 4 (e.g., complex I; Hagedorn et al., 2004). A reasonable value for K_C, or an estimate of how it changes between states 3 and 4, is not easily inferred. Consequently, in the following work, we do not constrain this parameter between states.

This leaves us with K_{NADH} and K_{NAD^+}. For these two parameters, the three simplest cases are considered: (1) both K_{NADH} and K_{NAD^+} are unchanged between states 3 and 4, (2) only K_{NADH} is changed, or (3) only K_{NAD^+} is changed. For each case, $n = 875$ μM (calculated as the average total NAD(H) in Table 3), and we explore a range of values for *e* (between 200 and 7000 μM). Using these values, the model is least-squares fitted to the data in Table 3 using an implementation of the Levenberg-Marquardt algorithm (More, 1977). A fit is considered as reproducing the data in Table 3 when $\chi^2 < 1$.

In case 1, keeping both K_{NADH} and K_{NAD^+} constant, it was not possible to reproduce the data. Thus, it is only possible to model the results in Figure 1 by changing the binding properties of NAD(H). In case 2, choosing an invariable medium binding strength ($K_{NAD^+} = 400\ M^{-1}$) similar to that determined previously (Hagedorn et al., 2004; Blinova et al., 2005) and varying K_{NADH}, the data in Table 3 were easily reproduced. The values for K_{NADH} determined by this fit are shown in Figure 3A. The ratio, $K_{NADH}(4)$: $K_{NADH}(3)$, lies between 2.5 and 3, as seen in Figure 3B. The absolute value of K_{NADH} depends on the total concentration of binding sites (which is unknown), but in general, a 2.5- to 3-fold reduction of the binding constant in state 3 reproduces the data in Table 3. In case 3, the data in Table 3 were not reproduced by any reasonable constant value for K_{NADH} (range tested 10^{-4} to $10^6\ M^{-1}$).

Thus, we conclude that a change in the binding properties of NAD^+, as calculated by the steady state model defined in Equations 1 to 5 (see Methods), cannot account for the experimental results. However, the data can by reproduced by changing the average binding of NADH to proteins in the matrix and on the inner surface of the inner mitochondrial membrane. We estimated that K_{NADH} should decrease 2.5 to 3 times in state 3 compared with state 4.

DISCUSSION

We have here shown that plant mitochondria contain two pools of NADH, free NADH, and protein-bound NADH. Bound NADH dominates in the absence of ADP (states 2 and 4), whereas free NADH is highest in the presence of ADP (state 3). However, the concentration of free NADH, the parameter determining the degree of interaction with enzymes, is surprisingly constant. Modeling shows that this observation can be explained by a decrease in the average binding of NADH to proteins by a factor of 2.5 to 3, whereas changes in NAD^+ binding cannot. The bound NADH is probably predominantly associated with the active site of oxidoreductase enzymes using it as a coenzyme. The mitochondrial matrix contains a number of abundant dehydrogenases, namely, pyruvate dehydrogenase, isocitrate dehydrogenase, 2-oxoglutarate dehydrogenase, MDH, and malic enzyme, as well as many less-abundant NADH binding enzymes. The total concentration of binding sites is probably in the low millimolar range similar to the concentration of NADH (Møller, 2001). Binding to other proteins, such as that observed for BSA (see Methods), which is probably nonspecific, cannot be excluded, but there is no

Table 5. Calculated Concentrations of Different NADH Species in Calibration Runs

Mixture	$[NADH]_{free}$ (μM)	$[NADH]_{bound}$ (μM)	$[ADH]_{free}$ (μM)
1	0.00	–	–
2	2.22	–	–
3	4.40	–	–
4	6.54	–	–
5	0.00	0.000	16.28
6	1.27	0.946	15.20
7	2.58	1.820	14.20
8	3.92	2.620	13.27

Concentrations of the stock solutions were determined spectrophotometrically. Measurements were done in a stirred open rank oxygraph vessel at a solution volume of 0.75 mL.

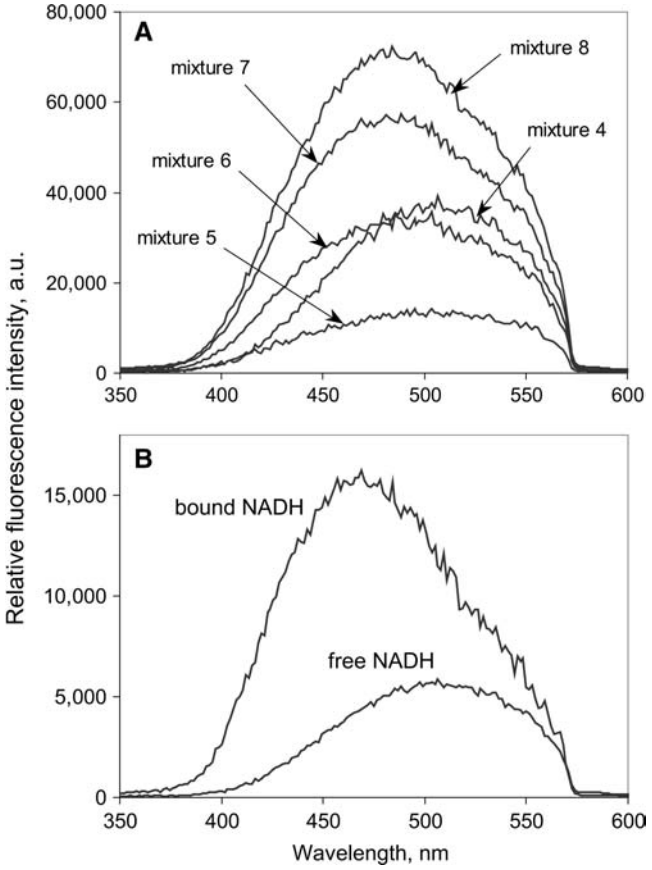

Figure 5. Decomposition of Standard Spectra into Three Components.

(A) Pseudo-steady-state emission spectra of mixtures of NADH and ADH in 5 mM HEPES, pH 7.5 (the exact compositions are given in Table 5).
(B) The base spectra of free and bound NADH used in the further decomposition of fluorescence spectra of potato tuber mitochondria. The spectrum of ADH is not shown. Uncorrected spectra are shown (see Figure 7).

evidence for such binding. There is however a fundamental difference between NADH bound to the active site of enzymes and nonspecifically bound NADH: The former is directly involved in metabolic processes (it has been caught in the act), whereas the latter constitutes an inactive pool.

The observation that free NADH in the mitochondrial matrix is maintained at a relatively constant level irrespective of respiratory state leads to two important conclusions: (1) The concentration of free NADH does not play a regulatory role in respiration. If it did, such a crude regulation would affect far too many processes simultaneously. Hence, it seems reasonable that the pool of free NADH is in homeostasis, while mitochondrial processes are regulated by other more specific mechanisms. (2) There is a specific mechanism for maintaining NADH homeostasis. Assuming that a steady state condition is reached at the end of each state, the binding affinity of the mitochondrial protein matrix must be dynamically adjusted during the respiratory cycle to keep the free NADH constant. Modeling shows that free NADH homeostasis is most likely due to changes in the binding properties of NADH, rather than NAD^+. According to our calculations, the average binding constant of NADH to mitochondrial proteins in state 3 should decrease by a factor of 2.5 to 3 relative to binding in state 4. One factor that can influence the enzyme–NADH interaction is the competitive binding of other metabolites or accumulation of reaction products. Another possible mechanism would be protein phosphorylation, which affects a number of the most active and abundant NAD(H) binding mitochondrial enzymes (Bykova et al., 2003) and which is higher in state 4 than in state 3 (Petit et al., 1990).

Here, we have demonstrated that potato tuber mitochondria contain an appreciable and fairly stable amount of free NADH in different metabolic states. Our data are in contrast with Wakita et al. (1995), who used kinetic analysis of the NADH fluorescence decay and were unable to detect free NADH in rat liver mitochondria irrespective of their respiratory state. Blinova et al. (2005), on the other hand, observed a high proportion of free NADH in pig heart mitochondria using a similar technique. These apparent discrepancies may reflect fundamental physiological differences between the role of free NADH in the mitochondria in their respective species and tissues.

Since 20% (state 4) to 60% (state 3 with succinate) of the total NADH is free in potato tuber mitochondria (Figures 1E and 2C), it means that the concentration of free NADH in the matrix is 100 to 150 μM or 50 to 75 μM, assuming a matrix volume of 1 or 2 μL/mg mitochondrial protein, respectively. One consequence of this is that because the concentration of free NADH is >3 times higher than the K_m (NADH) for both complex I and the rotenone-insensitive NADH dehydrogenase on the inner surface of the inner membrane of potato tuber mitochondria (Rasmusson and Møller, 1991), the rate of either enzyme will not be much limited by the NADH concentration. Therefore, their relative rates will be regulated by other factors, such as ADP availability,

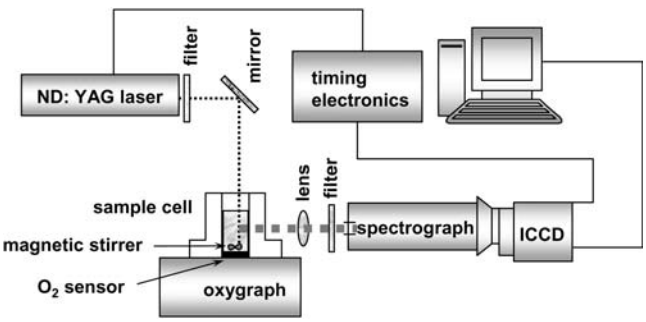

Figure 6. Drawing of the Time-Gated Fluorescence Setup, Showing How the Excitation Light from the Laser Is Directed toward the Sample Compartment.

The filter in front of the laser blocks higher wavelengths, allowing only 355-nm light to pass. The sample cell of an oxygen meter is equipped with magnetic stirring. The fluorescence signal is collected perpendicularly to the incident light. The filter in front of the spectrograph blocks wavelengths below 400 nm, thus effectively blocking the excitation light, allowing only the fluorescence spectrum to enter the spectrograph. The intensified charge-coupled device (ICCD) camera is coupled to the Q-switch of the laser through the timing unit, the controller, and the pulse generator.

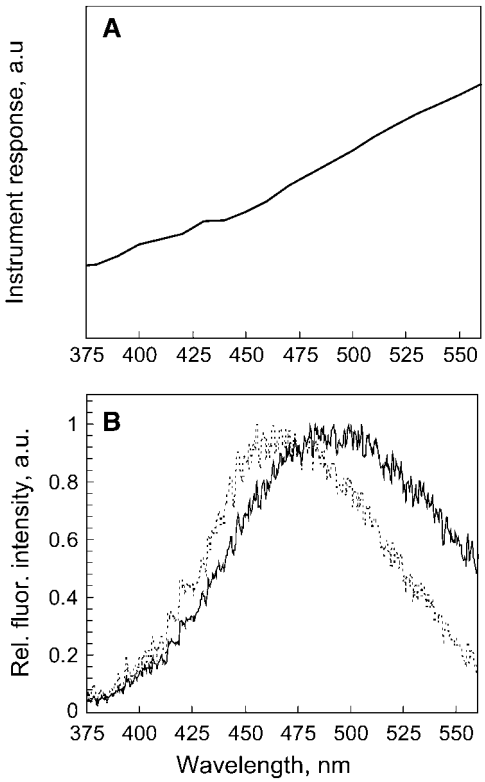

Figure 7. Spectral Data Correction.

(A) The instrument response function, showing the dependence of the sensitivity of our setup (see Figure 6) on the wavelength.
(B) Fluorescence emission spectrum of an NADH solution (free NADH) before (solid line) and after (dotted line) correction with the instrument response function. The correction shifts the emission maximum ~30 nm toward the blue.

posttranslational modifications, such as protein phosphorylation and/or protein oxidation, and the presence of as yet unknown effector molecules. Another consequence is that the free NADH:free NAD^+ ratio in the matrix will be at least 0.1 (more if an appreciable proportion of the NAD^+ is bound), and that is about two orders of magnitude higher than that estimated for the cytosol of plant cells (Heineke et al., 1991; Krömer and Heldt, 1991). This has important implications for the transport processes between the cytosol and the mitochondrial matrix. For example, it means that the malate/oxaloacetate transporter can only work to export reducing equivalents, which is thought to be important under photorespiratory conditions (Krömer and Heldt, 1991).

It will be interesting to apply the method for determining free and bound NADH developed here to isolated pea (*Pisum sativum*) leaf mitochondria, which differ in the following important aspects from potato tuber mitochondria.

Pea leaf mitochondria participate in photorespiration and therefore contain a very high concentration of the glycine decarboxylase complex (~0.2 mM NADH binding sites), which appears to have a high affinity for NADH. Binding of NADH to the glycine decarboxylase complex might decrease the amount of free NADH available to other enzymes and be one of the reasons why glycine is preferred over other mitochondrial respiratory substrates (Oliver et al., 1990; Møller, 2001). (1) The oxidation of Gly and malate by pea leaf mitochondria shows rather complex interactions, which have implications for their function in photorespiration (Wiskich et al., 1990). (2) Pea leaf mitochondria contain appreciable amounts of NADP(H), which can also vary significantly in reduction level (Agius et al., 2001; Igamberdiev and Gardeström, 2003). (3) Because they contain NADPH, the internal NADPH dehydrogenase might also be active in pea leaf mitochondria. This means that all three internal NAD(P)H dehydrogenases will be involved in reoxidizing NAD(P)H, making the regulation more complicated (Bykova and Møller, 2001; Møller, 2001; Rasmusson et al., 2004).

The method described here will also be applicable to other isolated organelles, intact cells, and perhaps even tissues. Knowledge about the proportion of free NAD(P)H in living tissues is crucial for interpreting their metabolic behavior. Since NAD(P)H is involved in detoxification of reactive oxygen species, the method might also provide a sensitive assay for oxidative stress.

METHODS

Materials

NADH, yeast ADH, fat-free BSA, and other chemicals were purchased from Sigma-Aldrich and were of the highest grade available.

Mitochondria were isolated from potato tubers (*Solanum tuberosum* cv Bintje) bought in the local market by differential centrifugation followed by Percoll density gradient centrifugation essentially as described by Struglics et al. (1993). The mitochondria oxidized malate (+Glu) at rates of 67 ± 12 nmol O_2/min × mg protein, respiratory controls of 5.6 ± 0.4, and ADP/O ratios of 2.1 ± 0.1 (means ± SD, $n = 3$ independent preparations). The corresponding numbers for succinate oxidation were 294 ± 32, 4.0 ± 0.6, and 1.3 ± 0.2, respectively.

Extraction and Quantification of Total Mitochondrial NAD(H)

Total NADH and NAD^+ was extracted from isolated potato tuber mitochondria and quantified by enzymatic assay essentially as described by Ciotti and Kaplan (1957).

Binding of NADH to Model Proteins

To decompose the spectra of POM into their free and bound components, the spectrum of NADH bound to mitochondrial proteins had to be obtained. Since NADH binds to a wide range of known and unknown proteins, this task cannot be accomplished without certain assumptions. To investigate how the spectrum of bound NADH depends on the binding strength, we first measured the binding parameters of several selected proteins by ITC. Furthermore, the spectral properties of these systems were studied by steady state and time-gated fluorescence. The model proteins included a mitochondrial MDH from pig heart and a nonmitochondrial protein with an NADH-specific binding site: yeast ADH. BSA has not been reported to have a specific binding site for NADH and was used as a model for nonspecific binding of NADH to proteins.

The calorimetric measurements were conducted with an MCS-ITC isothermal titration calorimeter (MicroCal) at 25°C. NADH and/or proteins were dissolved in 5 mM HEPES-KOH, pH 7.5. Concentrations of the proteins and NADH were determined spectrophotometrically using the published extinction coefficients ($\varepsilon_{340\ nm}$ [NADH] = 6.22 mM^{-1} cm^{-1} [Putnam, 1975]; $\varepsilon_{280\ nm}$ [pig heart mitochondrial MDH] = 39.2 mM^{-1} cm^{-1};

$\varepsilon_{280\ nm}$ [horse liver ADH] = 36.4 mM^{-1} cm^{-1}; $\varepsilon_{280\ nm}$ [yeast ADH] = 177.7 mM^{-1} cm^{-1}; $\varepsilon_{279\ nm}$ [BSA] = 44.31 mM^{-1} cm^{-1} [Hirayama et al., 1990]).

The protein solution, typically between 2 and 10 mg/mL, was loaded into the sample cell (V_{cell} = 1.3 mL) and titrated with a concentrated solution of NADH. The experiments were designed so that the amount of injected ligand at the end of a titration experiment was twice the number of potential binding sites of the protein. The results were fitted to a model with one set of independent binding sites. An example of a titration experiment for ADH is shown in Figure 4. The binding parameters were obtained by floating association constant (k_a), binding enthalpy (ΔH), and the number of binding sites (*n*). The obtained values for dehydrogenases (Table 4) are consistent with the literature (Subramanian and Ross, 1978). The association constants ranged from 10^4 (in the case of nonspecific binding to BSA) to 10^6 M^{-1}.

The studied dehydrogenases are believed to be dimers. However, most of the obtained numbers were consistently lower than two binding sites per dimer. This usually happens when some of the binding sites are inactive or occupied by another ligand. Our inability to obtain exactly two binding sites per dimer was probably due to the presence of some initial amount of NADH. This problem can be circumvented by the assumption that the number of available binding sites is smaller than the actual concentration of the protein. Adjusting down the concentration of the macromolecule gives the right number of binding sites but has no influence on the results of the fitting for the association constant. Therefore, the k_a and *n* obtained from ITC could be used directly in the treatment of the model system fluorescence data.

Spectra of Free and Bound NADH

The fluorescence of NADH in the presence of BSA or ADH shows that the environment of the binding site has a greater effect on the fluorescence intensity of the bound cofactor than on the spectral shift (data not shown). That is to say that binding to a nonspecific site (such as in BSA) shifts the emission maximum to the same extent as when NADH is bound to a specific site (as in case of ADH). The consequences of this effect on the outcome of the decomposition process are such that the amount of bound NADH can be overestimated or underestimated because the actual average binding constant of mitochondrial proteins is below or above the one assumed from the model system, respectively. However, the fact that the spectral shift is not greatly affected by the strength of binding ensures a proper estimation of the concentration of free NADH.

We selected yeast ADH as the model protein with an intermediate between specific and nonspecific binding properties for NADH. This model system was routinely tested prior to the beginning of the experiments with the mitochondria.

The spectrum of free NADH was measured directly on the solutions of pure NADH at different concentrations. The linearity of the fluorescence signal with the concentration of NADH was ensured using low concentrations (i.e., 1 to 10 μM). Using the binding parameters obtained from ITC, the concentrations of free and bound NADH were calculated for the three standard mixtures of NADH and ADH (Table 5, Figure 5A). These systems were designed to contain the same amount of total NAD(H) as our biological system, calculated with the assumption that the isolated mitochondria from potato tubers contain 1 to 2 nmol NAD(H) (mg protein)$^{-1}$ (Agius et al., 2001). Since we used 1 to 2 mg protein per mL in the assay, the maximum concentration of NADH in the assay would be 1 to 4 μM. The spectrum of bound NADH could be calculated from the spectra of the standard solutions (Figure 5B).

Decompositions of Mitochondrial Fluorescence Spectra

Decomposition was based on the notion that an experimental emission spectrum can be written as a linear superposition of the two emission spectra of free and bound NAD(P)H. Moreover, it was assumed that the emission spectrum of NAD(P)H bound to any protein closely resembles the emission spectrum of NADH bound to ADH. Specifically, spectra are nonnegative functions of frequency on the experimentally accessible frequency interval. Squared-integrable real functions on this interval form a vector space. The two emission spectra of free and bound NAD(P)H are two linearly independent vectors in this space. The experimental emission spectrum is a third vector in the same space and lies in the two-dimensional subspace spanned by the first two vectors if the experimental emission spectrum originates in free and bound NAD(P)H. Least-squares fitting of a linear combination of the first two spectra to the third vector (the experimental spectrum) yields the linear combination of the first two that differs the least from the latter. If the difference vanishes, one has a perfect decomposition. If it does not, the magnitude of the residual gives an estimate of the size of the error committed by claiming that the decomposition represents the experimental emission spectrum.

In practice, we represented the spectra by their values at 1100 frequency values. Then, a vector in the abstract function space is represented by an ordinary vector with 1100 real elements, and decomposition becomes matrix algebra: Emission spectra of the species free NADH and NADH bound to ADH (arranged in an 1100 $\times$ 2 matrix B) were calculated from emission spectra of *n* standard mixtures of NADH and ADH (in a 1100 $\times$ *n* matrix S) using the 2 $\times$ *n* matrix C of the NADH species concentrations in the standard mixtures as follows:

$$S = B \cdot C \qquad B = S \cdot C^T \cdot (C \cdot C^T)^{-1}.$$

The species concentrations in C were calculated from total amounts of NADH and ADH and the binding constant of NADH and number of NADH binding sites on ADH obtained by ITC.

Concentrations of the NADH species in a series of *m* experimental emission spectra (arranged in an 1100 $\times$ *m* matrix Z) were then calculated by writing each column in Z as a linear combination of the two columns in B and a vector orthogonal to those two columns. Doing this for all *m* spectra in Z, there are *m* orthogonal vectors. These can be arranged in a residual matrix R, so in matrix form one has the following:

$$Z = B \cdot D \qquad D = (B^T \cdot B)^{-1} \cdot B^T \cdot Z.$$

This decomposition of experimental spectra in Z after the two spectra in B is equivalent with least-squares fitting of a linear superposition of the two spectra in B to each of the spectra in Z. The parameters fitted are the elements of D, and their resulting values are those given in the identity for D above. The quality of this fit was evaluated by inspection of the residual spectra arranged in the 1100 $\times$ *m* matrix R as follows:

$$R = Z - B \cdot D.$$

Fluorescence Measurements

The fluorescence instrument was developed on site specifically for investigating NADH turnover in biological samples (Figure 6). Briefly, fluorescence was induced by the third harmonic of a Q-switched Nd:YAG laser (Continuum) at 355 nm. The laser pulse width was 5 ns with 1-ns jitter, and the pulse repetition rate was 10 Hz. Fluorescence emission was detected through the transparent wall of an oxygraph sample cell perpendicular to the incident light. The emitted light was collected on the entrance slit of a Jobin Yvon spectrometer and then detected by an ICCD camera composed of a lens-coupled microchannel plate image intensifier and a liquid nitrogen cooled CCD detector, both from Princeton Instruments. The controller (ST-128)/pulse generator (PG-200) unit (both from Princeton Instruments) coordinated the onset of a laser pulse and

the delayed data collection, which was triggered by the Q-switch of the laser. The gate width was 20 ns centered at the peak of the laser pulse intensity, thus ensuring equilibrium between the excitation and the emission processes. Such a data collection window allows determination of the ''steady state'' data, where the quotation marks indicate a certain approximation of the term, when applied to our method.

There are two advantages to the use of a pulsed excitation regime: (1) Bleaching is reduced, and (2) it allows collection of time-gated data in addition to the steady state spectra. Expanding the method initially introduced by Paul and Schneckenburger (1996), we made a series of measurements of NADH fluorescence lifetimes in different metabolic states. The measurements of fluorescence decays have an advantage over the steady state measurements because the fluorescence lifetime of bound NADH is an order of magnitude longer than that of a free NADH (see Introduction). Consistent with this, our preliminary results indicated that the observed fluorescence of potato mitochondria has a longer lifetime in those states that have an increased proportion of bound NADH. Quantification of this qualitative result, however, requires a rigorous mathematical treatment not attempted in this study and points toward further possible improvement of our method.

Calibration of the wavelength scale of the spectrometer was conducted prior to the experiments. Correction of the fluorescence emission intensity to the instrument response function was performed only once to ensure the correct location and shape of the NADH fluorescence. This is shown in Figure 7, and the excitation peak in the corrected spectrum was shifted ~30 nm compared with the uncorrected spectrum. In the experiments presented in Figures 1B, 1C, and 5, the fluorescence emission data were not corrected, which resulted in no loss of generalization in data interpretation.

Modeling

It is assumed that NADH and NAD^+ bind reversibly to the same pool of binding sites, E, that is

$$\mathrm{E} + \mathrm{NADH} \rightleftharpoons \mathrm{ENADH} \quad \text{(a)}$$

$$\mathrm{E} + \mathrm{NAD}^+ \rightleftharpoons \mathrm{ENAD}^+, \quad \text{(b)}$$

where ENADH and $ENAD^+$ denote the bound NADH and bound NAD^+, respectively. In the matrix, NADH is converted to NAD^+ by complex I and ND_{in}, and NAD^+ is converted back to NADH by (primarily) malic enzyme and MDH. We need not consider the details of these enzymatic reactions if we simply assume that the system has reached a steady state (no change in concentration over time at the time points considered). Consequently, the conversions are written simply as

$$\mathrm{NADH} \rightleftharpoons \mathrm{NAD}^+. \quad \text{(c)}$$

At steady state, Reactions a to c can be written as the following equations:

$$K_{\mathrm{NADH}} = [\mathrm{ENADH}]/[\mathrm{E}][\mathrm{NADH}] \quad (1)$$

$$K_{\mathrm{NAD}^+} = [\mathrm{ENAD}^+]/[\mathrm{E}][\mathrm{NAD}^+] \quad (2)$$

$$K_{\mathrm{C}} = [\mathrm{NAD}^+]/[\mathrm{NADH}], \quad (3)$$

where the brackets around the compounds denote equilibrium concentrations, and K_{NADH}, K_{NAD^+}, and K_C are the equilibrium constants. Reactions a to c imply that the total concentration of binding sites (e) and the total concentration of NAD(H) (n) are constant:

$$[\mathrm{E}] + [\mathrm{ENADH}] + [\mathrm{ENAD}^+] = e \quad (4)$$

$$[\mathrm{NADH}] + [\mathrm{NAD}^+] + [\mathrm{ENADH}] + [\mathrm{ENAD}^+] = n \quad (5)$$

Equations 1 to 5 constitute five equations, with five parameters (K_{NADH}, K_{NAD^+}, K_C, e, and n) and five concentrations ([NADH], [NAD^+], [E], [ENADH], and [$ENAD^+$]).

Combination of Equations 1 to 5 yields the equations from which [NADH] (or [E]) can be calculated:

$$\begin{cases} e = [\mathrm{E}] \cdot (1 + K \cdot [\mathrm{NADH}]) \\ n = [\mathrm{NADH}] \cdot (L + K \cdot [\mathrm{E}]) \end{cases}$$

with

$$\begin{cases} K = K_{\mathrm{NADH}} + K_{\mathrm{C}} K_{\mathrm{NAD}^+} \\ L = 1 + K_{\mathrm{C}} \end{cases}.$$

The solution for [NADH] is as follows:

$$[\mathrm{NADH}] = \frac{-\{L + K(e-n)\} + \sqrt{\{L + K(e-n)\}^2 + 4nKL}}{2KL}.$$

The other concentrations follow from this.

ACKNOWLEDGMENTS

We thank Ina Blom for excellent technical assistance, Peter Westh for loan of the ITC instrument, Søren K. Rasmussen and Steen G. Hanson for continuous support, and the following organizations and agencies for economic support: Center for Biomedical Optics and CIRIUS, Danish Ministry of Education, to J.G., Danish Natural Science Research Council to I.M.M., and Risø National Laboratory to M.R.K., P.E.A., and I.M.M.

Received November 9, 2005; revised December 22, 2005; accepted January 9, 2006; published February 3, 2006.

REFERENCES

Agius, S.C., Rasmusson, A.G., and Møller, I.M. (2001). NAD(P) turnover in plant mitochondria. Aust. J. Plant Physiol. **28,** 461–470.

Avi-Dor, Y., Olson, J.M., Doherty, M.D., and Kaplan, N.O. (1962). Fluorescence of pyridine nucleotides in mitochondria. J. Biol. Chem. **237,** 2377–2383.

Blinova, K., Carroll, S., Bose, S., Smirnov, A.V., Harvey, J.J., Knutson, J.R., and Balaban, R.S. (2005). Distribution of mitochondrial NADH fluorescence lifetimes: Steady-state kinetics of matrix NADH interactions. Biochemistry **44,** 2585–2594.

Bykova, N.V., Egsgaard, H., and Møller, I.M. (2003). Identification of 14 new phosphoproteins involved in important plant mitochondrial processes. FEBS Lett. **540,** 141–146.

Bykova, N.V., and Møller, I.M. (2001). Involvement of matrix NADP turnover in the oxidation of NAD^+-linked substrates by pea leaf mitochondria. Physiol. Plant. **111,** 448–456.

Ciotti, M.M., and Kaplan, N.O. (1957). Procedures for determination of pyridine nucleotides. Methods Enzymol. **3,** 890–899.

Duysens, L.N.M., and Kronenberg, G.H.M. (1957). The fluorescence spectrum of the complex of reduced phosphopyridine nucleotide and alcohol dehydrogenase from yeast. Biochim. Biophys. Acta **26,** 437–438.

French, S.A., Territo, P.R., and Balaban, R.S. (1998). Correction for

inner filter effects in turbid samples: Fluorescence assays of mitochondrial NADH. Am. J. Physiol. **275,** C900–C909.

Gafni, A., and Brand, L. (1976). Correction for inner filter effects in turbid samples: Fluorescence assays of mitochondrial NADH. Biochemistry **15,** 3165–3171.

Hagedorn, P.H., Flyvbjerg, H., and Møller, I.M. (2004). Modelling NADH turnover in plant mitochondria. Physiol. Plant. **120,** 1–16.

Heineke, D., Riens, B., Grosse, H., Hoferichter, P., Peter, U., Flügge, U.-I., and Heldt, H.W. (1991). Redox transfer across the inner chloroplast envelope membrane. Plant Physiol. **95,** 1131–1137.

Hirayama, K., Akashi, S., Furuya, M., and Fukuhara, K. (1990). Rapid confirmation and revision of the primary structure of bovine serum albumin by ESIMS and Frit-FAB LC/MS. Biochem. Biophys. Res. Commun. **173,** 639–646.

Igamberdiev, A.U., and Gardeström, P. (2003). Regulation of NAD- and NADP-dependent isocitrate dehydrogenases by reduction levels of pyridine nucleotides in mitochondria and cytosol of pea leaves. Biochim. Biophys. Acta **1606,** 117–125.

Krömer, S., and Heldt, H.W. (1991). Respiration of pea leaf mitochondria and redox transfer between the mitochondrial and extramitochondrial compartment. Biochim. Biophys. Acta **1057,** 42–50.

Lakowics, J.R., Szmacinski, H., Nowaczyk, K., and Johnson, M.L. (1992). Fluorescence lifetime imaging of free and protein-bound NADH. Proc. Natl. Acad. Sci. USA **89,** 1271–1275.

Langan, T.A. (1960). Changes in the fluorescence spectrum of reduced triphosphopyridine nucleotide on binding to isocitric dehydrogenase. Acta Chem. Scand. A **14,** 936–938.

Møller, I.M. (2001). Plant mitochondria and oxidative stress. Electron transport, NADPH turnover and metabolism of reactive oxygen species. Annu. Rev. Plant Physiol. Plant Mol. Biol. **52,** 561–591.

Møller, I.M., and Lin, W. (1986). Membrane-bound NAD(P)H dehydrogenses in higher plant cells. Annu. Rev. Plant Physiol. **37,** 309–334.

Møller, I.M., and Palmer, J.M. (1982). Direct evidence for the presence of a rotenone-resistant NADH dehydrogenase on the inner surface of the inner membrane of plant mitochondria. Physiol. Plant. **54,** 267–274.

Moore, A.L., Dry, I.A., and Wiskich, J.T. (1988). Measurement of the redox state of the ubiquinone pool in plant mitochondria. FEBS Lett. **235,** 76–80.

More, J.J. (1977). The Levenberg-Marquardt algorithm: Implementation and theory. In Numerical Analysis, Lecture Notes in Mathematics, Vol. 630. G. Watson, ed (Berlin: Springer-Verlag), pp. 105–116.

Neuburger, M., Day, D.A., and Douce, R. (1984). The regulation of malate oxidation in plant mitochondria by the redox state of endogenous pyridine nucleotides. Physiol. Veg. **22,** 571–580.

Nicholls, D.G., and Ferguson, S.J. (2002). Bioenergetics 3. (Amsterdam: Academic Press).

Oliver, D.J., Neuburger, M., Bourgignon, J., and Douce, R. (1990). Glycine metabolism by plant mitochondria. Physiol. Plant. **80,** 487–491.

Palmer, J.M., Schwitzguebel, J.-P., and Møller, I.M. (1982). Regulation of malate oxidation in plant mitochondria. Response to rotenone and exogenenous NAD^+. Biochem. J. **208,** 703–711.

Paul, R.J., and Schneckenburger, H. (1996). Oxygen concentration and the oxidation-reduction state of yeast: Determination of free/bound NADH and flavins by time-resolved spectroscopy. Naturwissenschaften **83,** 32–35.

Petit, P.X., Sommarin, M., Pical, C., and Møller, I.M. (1990). Modulation of endogenous protein phosphorylation in plant mitochondria by respiratory substrates. Physiol. Plant. **80,** 493–499.

Putnam, F.W., ed (1975). The Plasma Proteins: Structure, Function, and Genetic Control. (New York: Academic Press), pp. 1, 141, 147.

Rasmusson, A.G., and Møller, I.M. (1991). NAD(P)H dehydrogenases on the inner surface of the inner mitochondrial membrane studied using inside-out submitochondrial particles. Physiol. Plant. **83,** 357–365.

Rasmusson, A.G., Soole, K.L., and Elthon, T.E. (2004). Alternative NAD(P)H dehydrogenases of plant mitochondria. Annu. Rev. Plant Biol. **55,** 23–39.

Scott, T.G., Spencer, R.D., Leonard, N.J., and Weber, G. (1970). Emission properties of NADH. Studies of fluorescence lifetimes and quantum efficiencies of NADH, AcPyADH, and simplified synthetic models. J. Am. Chem. Soc. **92,** 687–695.

Stocchi, V., Cucchiarini, L., Magnani, M., Chiarantini, L., Palma, P., and Cresentini, G. (1985). Simultaneous extraction and reversed-phase high performance liquid chromatographic determination of adenine and pyridine nucleotides in human blood cells. Anal. Biochem. **146,** 118–124.

Struglics, A., Fredlund, K.M., Rasmusson, A.G., and Møller, I.M. (1993). The presence of a short redox chain in the membrane of potato tuber peroxisomes and the association of malate dehydrogenase with the membrane. Physiol. Plant. **88,** 19–28.

Subramanian, S., and Ross, P.D. (1978). Thermodynamics of binding of oxidized and reduced nicotinamide adenine dinucleotides, adenosine-5′-diphosphoribose, and 5′-iodosalicylate to dehydrogenases. Biochemistry **17,** 2193–2197.

Wakita, M., Nishimura, G., and Tamura, M. (1995). Some characteristics of the fluorescence lifetime of reduced pyridine nucleotides in isolated mitochondria, isolated hepatocytes, and perfused rat liver *in situ*. J. Biochem. (Tokyo) **118,** 1151–1160.

Wiskich, J.T., Bryce, J.H., Day, D.A., and Dry, I.B. (1990). Evidence for metabolic domains within the matrix compartment of pea leaf mitochondria. Plant Physiol. **93,** 611–616.